Eur. Phys. J. D **6**, 375–381 (1999)

THE EUROPEAN PHYSICAL JOURNAL D

EDP Sciences

Storage ring free electron laser dynamics, with the inclusion of bunch lengthening and energy spread increasing effects

G. Dattoli[a], L. Mezi, M. Migliorati[b], and A. Renieri

ENEA - Dipartimento Innovazione, Divisione Fisica Applicata, Centro Ricerche di Frascati
C.P. 65 - 00044 Frascati, Rome, Italy

Received: 31 March 1998 / Received in final form: 16 September 1998

Abstract. We develop a rate equation model of the Storage Ring Free Electron Laser dynamics, which includes bunch lengthening and energy spread increasing effects, due to the combined mechanism of potential well distortion and collective random excitations. The model is based on the ordinary storage ring Free Electron Laser equations, coupled to Haissinski-type equations, accounting for the previously quoted effects. The obtained results are shown to provide a reliable tool, yielding a transparent understanding of the interplay between Free Electron Laser and e-beam induced effects.

PACS. 29.20.Dh Storage rings – 41.60.Cr Free-electron lasers

1 Introduction

The Storage Ring Free Electron Laser (SR-FEL) dynamics is a partially understood topic. The main aspects have been clarified by the pioneering papers [1–3] on the subject, which were able to provide a clear understanding of the interplay between FEL interaction induced e-beam energy spread, damping and saturation. Subsequent experimental work [4,5] confirmed these mechanisms and more recent investigations [6] have also confirmed the existence of stationary mode structures of the super-mode type, suggested in references [3,7,8].

A complete understanding of SR-FEL dynamics demands for a deeper insight into the interplay between the FEL and the mechanisms leading to the SR e-beam instabilities. Experimental observations [9,10] provided unexpected conclusions. They seem to suggest that, under given conditions, the FEL may induce a stabilizing feedback mechanism for instabilities yielding anomalous bunch lengthening [11] and head tail effects [12]. Preliminary theoretical investigations [13,14] have provided a first understanding of the mechanisms underlying the above-quoted phenomenology. We remind, indeed, that the microwave instability and the consequent increase of bunch length and energy spread are counteracted, according to reference [13], by the FEL-induced energy-dependent energy spread and by the modification of the longitudinal damping times [15]. The stabilizing effect of the head-tail instabilities occurs through a mechanism involving the FEL gain and modification of the instability growth rate due to e-bunch lengthening induced by the FEL interaction itself. This paper is devoted to the development of a simple dynamical model of a FEL oscillator allowing the inclusion of potential well distortion and turbulence effects. The model we develop is a combination of SR-FEL rate equations, with a semianalytical description of the above-quoted affects, which reduces the problem to the solution of algebraic equations, yielding bunch length and energy spread in terms of the main machine parameters.

Before entering into the specific details of the problem, let us remind the basic tools of the SR-FEL rate equations analysis [16,17]. The dynamical behavior of this type of device can be summarized as follows. An e-bunch is passed many times through the optical cavity where emits and amplifies coherent radiation, in this process the electrons undergoes a diffusion effect which induces an energy spread and a bunch lengthening, which is in turn responsible for a reduction of the peak current. The consequent gain reduction provides the switch off of the laser process. When the FEL is no more active, the natural damping mechanism restores the starting beam conditions so that the lasing process may start again.

According to the above description the equations modeling the SR-FEL dynamics can be written as [17]

$$\frac{\mathrm{d}}{\mathrm{d}\tau}y = \frac{y\tau_s}{T}\left[\frac{1}{(1+\widetilde{\sigma}^2)^{0.5}}\frac{1}{[1+1.7\mu_e(0)^2(1+\widetilde{\sigma}^2)]} - r\right],$$
$$\frac{\mathrm{d}}{\mathrm{d}\tau}\widetilde{\sigma}^2 = -2(\widetilde{\sigma}^2 - y), \quad \tau = \frac{t}{\tau_s}. \tag{1}$$

In equation (1) τ is a dimensionless time normalized to the damping time τ_s, y is the dimensionless intracavity optical power, $\widetilde{\sigma}$ is the ratio between induced and natural

[a] e-mail: dattoli@frascati.enea.it

[b] *Permanent address*: Università di Roma "la Sapienza" and LNF-INFN Frascati, Italy

energy spread $\sigma_\varepsilon(0)$ and

$$\mu_\varepsilon(0) = 4N\sigma_\varepsilon(0) \tag{2}$$

is the associated inhomogeneous broadening coefficient, r is linked to the cavity losses and T to the machine revolution period. The first equation accounts for the intracavity evolution intensity, the second for the induced energy spread characterized by an increase due to the intracavity power and by a reduction induced by the radiative damping. It is worth noting that the term $\frac{1}{(1+\widetilde{\sigma}^2)^{0.5}}$ accounts for the degradation due to the induced bunch lengthening, while $\frac{1}{[1+1.7\mu_e(0)^2(1+\widetilde{\sigma}^2)]}$ for that due to the induced energy spread.

Equations (1, 2) take into account the SR longitudinal dynamics based on the ordinary radiative equilibrium theory [18], possible modifications due to other effects have not been considered within the framework of this type of model.

The paper consists of four sections and one appendix. In Section 2 we treat the combined effects of FEL and potential well distortion, Section 3 is devoted to the problem of "Anomalous Turbulent Contributions", finally Section 4 contains concluding remarks and comparison to earlier works. The Appendix is addressed to the details of the notation and to numerical estimates of the parameters exploited in the main body of the paper.

2 FEL and potential well distortion

As already stated in the introductory section, this paper contains an analysis of the mutual feedback between FEL and SR longitudinal dynamics, with the inclusion of effects that yield length and relative energy spread of the e-bunches larger than those predicted by the ordinary radiative equilibrium theory [18]. These effects are due to the coupling of the e-beam with the vacuum pipe and the cases we will consider are those relevant to potential well distortion and microwave instability. The first effect is characterized by an increase of the bunch length without appreciable variations of the energy spread, the second also known as anomalous bunch lengthening is characterized by an increase of both bunch length and energy spread.

The so-called potential well distortion (p.w.d.) [19] is caused by a modification in the potential of the accelerating voltage, induced by the short range e.m. fields produced by the interaction of a bunch with the vacuum chamber and machine devices. A consequence of p.w.d. is an increase of the bunch length, which can be derived from the so-called Haissinski equation, an integral equation which under the assumption of inductive wake-fields and parabolic bunch distribution, leads to

$$\left(\frac{\sigma_z}{\sigma_{z,0}}\right)^3 - \left(\frac{\sigma_z}{\sigma_{z,0}}\right) - \frac{A}{\sigma_{z,0}^3} = 0\,, \qquad A = \lambda I_0 \frac{z_i}{n}\,, \tag{3a}$$

where I_0 is the average electron bunch current and $z_{i/n}$ the broad-band impedance of the machine evaluated at a characteristic frequency $\omega_c = n\omega_0$ with ω_0 the revolution frequency and $n = \frac{L_c}{2\pi\sigma_z}$ with L_c being the ring circumference. The parameter λ is a quantity depending on the other characteristic machine parameters (for details see the appendix). We have denoted by $\sigma_{z,0}$ the natural e-bunch length, *i.e.* that which in the absence of the p.w.d. effect is linked to the natural relative energy spread by

$$\sigma_{z,0} = \frac{c\alpha_c}{\omega_s}\sigma_\varepsilon^0\,, \tag{3b}$$

where α_c is the momentum compaction, ω_s the synchrotron frequency.

The important point to be stressed is that the p.w.d. induces a modification of the bunch length and not of the energy spread. We can therefore study the modification in the FEL dynamics due to the p.w.d. according to the following self-consistency loop:

a) The FEL induces an energy spread which combines quadratically to the natural energy spread.
b) The new energy spread can be exploited through equations (1) to determine the bunch length, due to the combined effect of the FEL and the p.w.d.
c) Both energy spread and bunch length can be exploited to determine the FEL gain.

To describe the evolution of the system dynamics, we use equations (1) which are still valid, provided that the first is replaced by

$$\frac{\mathrm{d}y}{\mathrm{d}\tau} = \frac{y\tau_s}{T}\left[\frac{1}{R(\widetilde{\sigma})}\frac{1}{[1+1.7\mu_\varepsilon^2(0)(1+\widetilde{\sigma}^2)]} - r\right], \tag{4}$$

where

$$R(\widetilde{\sigma}) = \frac{\overline{\sigma}_z(\widetilde{\sigma})}{\overline{\sigma}_z(0)} \tag{5}$$

and $\overline{\sigma}_z(\widetilde{\sigma})$ is the root of the equation

$$\overline{\sigma}_z^3 - (1+\widetilde{\sigma}^2)\overline{\sigma}_z - \bar{A} = 0, \quad \overline{\sigma}_z = \left(\frac{\sigma_z}{\sigma_{z,0}}\right), \quad \bar{A} = A/\sigma_{z,0}^3\,. \tag{6}$$

The term containing $\frac{1}{R(\widetilde{\sigma})}$ accounts for the FEL-induced effects combined to those due to the p.w.d.

The result of the numerical integration of equations (2-4) is provided in Figures 1, 2 for the parameters of Table 1. It is evident that when the p.w.d. is active ($A \neq 0$), the laser stationary power is larger than the case without p.w.d. The reason is presumably due to the fact that in the presence of p.w.d. the system is less sensitive to bunch length variation as shown in Figure 2, where we have reported the induced bunch lengthening *vs.* $\widetilde{\sigma}^2$ for the cases with and without p.w.d.

The stationary output power can be obtained from the equation [17]

$$E(r, \mu_\varepsilon(0)) = 1.422\, r\mu_\varepsilon^2(0) X(r, \mu_\varepsilon(0))\,, \tag{7}$$

which defines the system efficiency, the quantity X obtained from the equation

$$R(X)[1 + 1.7\mu_\varepsilon^2(0)(1+X)] = \frac{1}{r}\,. \tag{8}$$

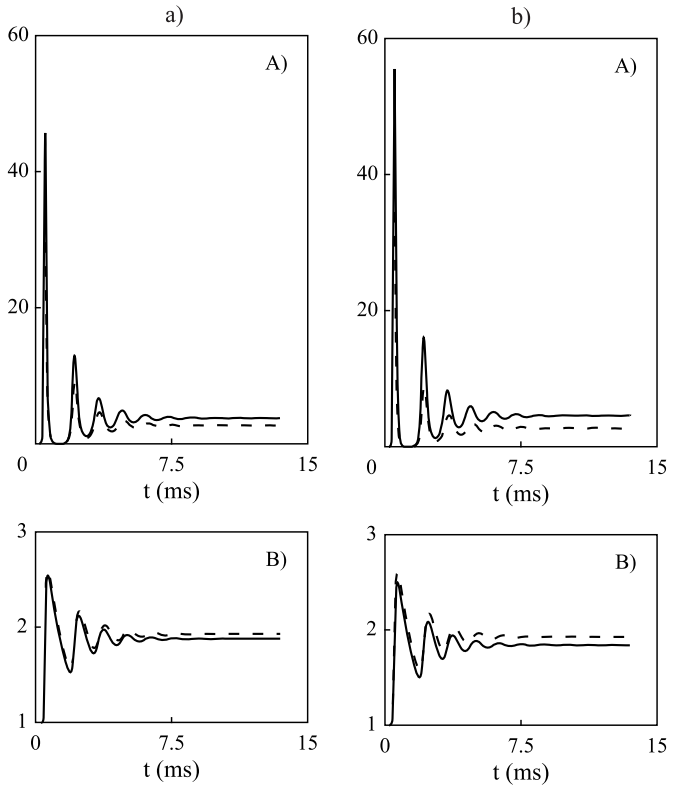

Fig. 1. a) A) Intracavity power evolution *vs.* t for a SR-FEL with (continuous line) and without (dotted line) p.w.d. B) Evolution of the FEL-induced bunch lengthening normalized to the initial bunch length *vs.* t. In both cases we have taken $\bar{A} = 0.5$ (for the other parameters see Tab. 1). b) Same as a) for $\bar{A} = 1$.

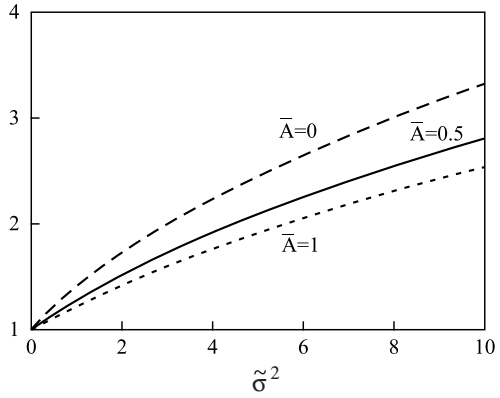

Fig. 2. FEL bunch lengthening normalized to the initial bunch length *vs.* $\tilde{\sigma}^2$ for different values of $\bar{A}$.

In Figures 3, 4, 5 we have reported the stationary intracavity power *vs.* r at fixed $\mu_\varepsilon(0)$ and $\bar{A}$. It is evident that in any case the output stationary power is larger when p.w.d. is active.

Further comments will be presented in the concluding section.

Table 1. T is not the machine revolution period but the machine revolution period normalized to the peak gain.

τ_s	=	$1.5 \cdot 10^{-3}$ s
r	=	0.47
T	=	$1.176 \cdot 10^{-5}$ s
$\sigma_\varepsilon(0)$	=	$8 \cdot 10^{-4}$
N	=	40

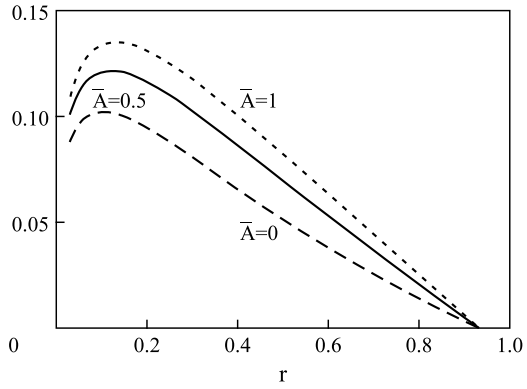

Fig. 3. Efficiency function *vs.* r for different $\bar{A}$ values and fixed $\mu_\varepsilon(0) = 0.2$.

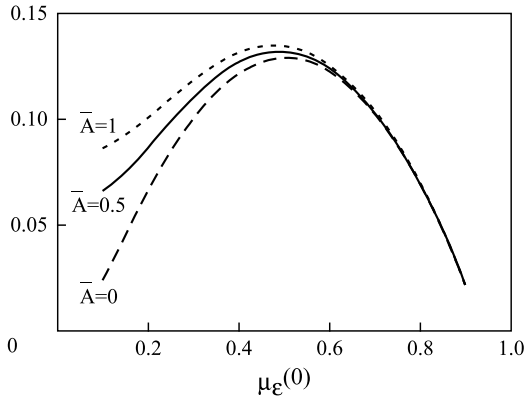

Fig. 4. Same as Figure 3 *vs.* $\mu_\varepsilon(0)$ for different $\bar{A}$ values and fixed $r = 0.4$.

3 FEL bunch lengthening and energy spread increasing effects

In the previous section we have considered a case in which the mechanisms, modifying the beam parameters with respect to the natural values, leave the energy spread unaffected.

However, when the bunch current gets larger, one may have either bunch lengthening and energy spread increasing. The phenomenon has been explained as the occurrence of a longitudinal instability due to the coupling of the electrons with the SR environment, like electrodes and spurious cavities. The items responsible for this instability are resonating at high frequencies (typically in the microwave region) with frequencies in the GHz range. The relevant wavelengths are therefore short compared

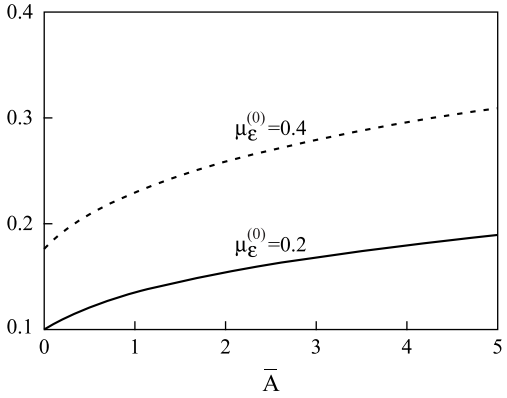

Fig. 5. Same as Figure 3 *vs.* $\bar{A}$ for fixed $r = 0.15$ and different $\mu_\varepsilon(0)$ values.

to the electron bunch length and the instability is therefore a single bunch effect without any machine turn by turn memory. This effect, called anomalous or turbulent bunch lengthening cannot be explained in terms of the Haissinski treatment, since the bunch distribution is not constant anymore. A more appropriate analysis requires the direct solution of the Fokker-Planck equation [20] in the time domain, or the use of numerical simulations [21]. In both cases a numerical treatment, requiring large computer time, is necessary. In the following we will use the analysis developed in reference [22], which allows to evaluate bunch length and energy spread from the modified Haissinski equations

$$\left(\frac{\sigma_z}{\sigma_{z,0}}\right)^3 - \left(\frac{\sigma_z}{\sigma_{z,0}}\right)\left[1 + B\left(\frac{\sigma_{z,0}}{\sigma_z}\right)^{2a}\right] - \frac{A}{\sigma_{z,0}^3} = 0\,,$$
$$\left(\frac{\sigma_\varepsilon}{\sigma_{\varepsilon,0}}\right)^2 = 1 + B\left(\frac{\sigma_{z,0}}{\sigma_z}\right)^{2a}\;; \qquad (9)$$
$$B = l_1 I_0^2 K_e^2(\sigma_{z,0})\,.$$

The physical origin of the new contributions depending on the B factor which in turn depends on the loss factor $K_e(\sigma_{z,0})$ (for further details see the appendix) can be traced back to nonlinearities of the wake fields. Furthermore the maximum amplitude of the last contribution has been assumed to be proportional to the loss factor, whose dependence on the bunch length has been parametrized as $(\frac{\sigma_{z,0}}{\sigma_z})^a$. As to the value of a, it has been pointed out that it is specific for the machine under consideration. By using for example the scaling law which has first been applied to the machine SPEAR [23], we have $a \cong 1.21$. (For further details see the appendix.)

Independently of the physical explanation of the contribution to the energy spread due to the B factor in equations (8), we want to remark that the model gives a behaviour of bunch length and energy spread *vs.* current in agreement with those measured in different machines [22], and in our case such an algebraic approach is sufficient for studying the interaction with the FEL.

The SR-FEL rate equations of the previous section require slight modifications, the second of equations (1)

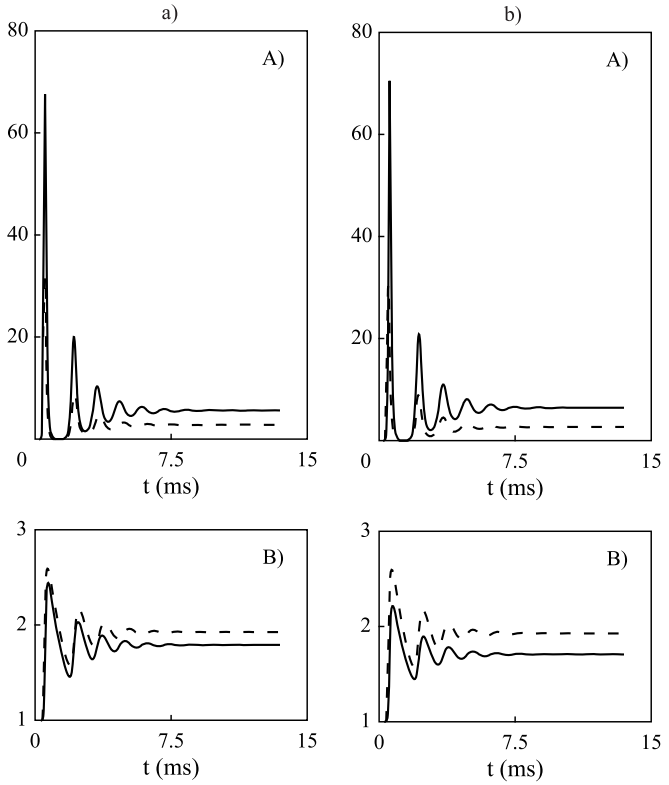

Fig. 6. a) Same as Figure 1 for $\bar{A} = 0.5$ $B = 8$, $a = 3$. b) Same as Figure 1 for $\bar{A} = 1$, $B = 15$, $a = 2$.

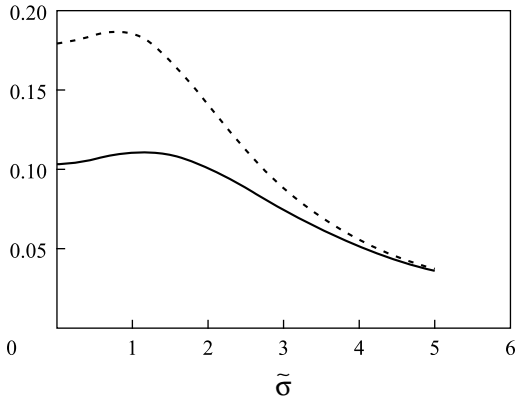

Fig. 7. $\alpha(\tilde{\sigma})/B$ *vs.* $\tilde{\sigma}$. Dashed line: $\bar{A} = 0.1$, $B = 20$, $a = 2$. Solid line: $\bar{A} = 0.1$, $B = 4$, $a = 2$.

holds unchanged while the first should read

$$\frac{\mathrm{d}y}{\mathrm{d}\tau} = \frac{y\tau_s}{T}\left[\frac{1}{R(\tilde{\sigma})}\frac{1}{[1+1.7\mu_\varepsilon^2(0)\,(\Sigma(\tilde{\sigma}))^2]} - r\right], \qquad (10)$$

where $\Sigma(\tilde{\sigma})$ is provided by

$$\Sigma(\tilde{\sigma}) = \left[(1+\tilde{\sigma}^2)\left(1 + \frac{B}{\overline{\sigma}_z(\tilde{\sigma})^{2a}}\right)\right]^{0.5} \qquad (11)$$

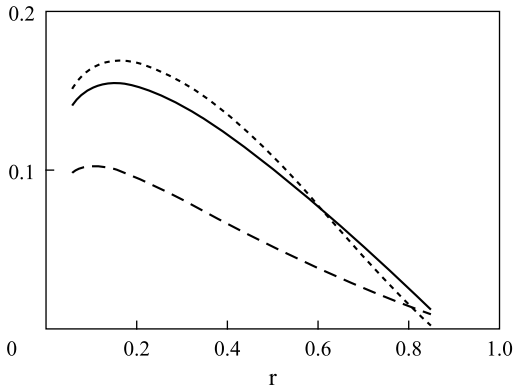

Fig. 8. Efficiency function *vs.* r. Long-dashed line: $\bar{A} = 0$, $\mu_\varepsilon(0) = 0.2$. Solid line: $\bar{A} = 0.5$, $\mu_\varepsilon(0) = 0.2$, $B = 30$, $a = 3$. Dashed line: $\bar{A} = 1$, $\mu_\varepsilon(0) = 0.2$, $B = 8$, $a = 3$.

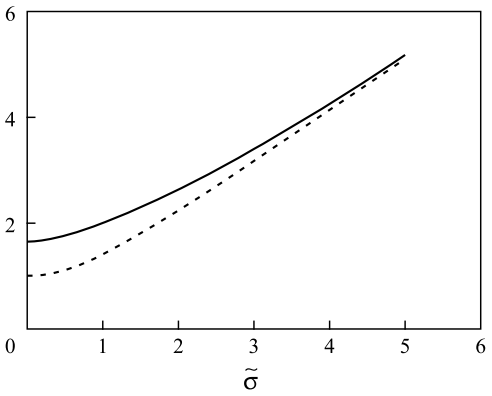

Fig. 9. Induced energy spread normalized to the natural energy spread *vs.* $\widetilde{\sigma}$. Solid line: $\bar{A} = 1$, $B = 20$, $a = 2$. Dashed line: $\bar{A} = B = 0$ (natural case).

and $\overline{\sigma}_z(\widetilde{\sigma})$ is the root of

$$\overline{\sigma}_z^3 - (1+\widetilde{\sigma}^2)\left(1 + \frac{B}{\overline{\sigma}_z(\widetilde{\sigma})^{2a}}\right)\overline{\sigma}_z - \bar{A} = 0\,. \tag{12}$$

The results of the numerical analysis are shown in Figures 6. It is evident that in this case too the stationary output power of the FEL operating with the beam having longer bunch and larger energy spread is larger or equivalent to that of the natural case. The explanation of this fact comes from Figure 7 where we have plotted the quantity

$$\alpha(\widetilde{\sigma}) = \frac{(1+\widetilde{\sigma}^2)}{\overline{\sigma}_z(\widetilde{\sigma})^{2a}} B\,, \tag{13}$$

representing the contribution of the anomalous bunch length to the FEL-induced energy spread. The adjective anomalous remarks the difference in bunch length and energy spread with respect to the values predicted by the equilibrium between radiation damping and quantum fluctuations. It is evident that for increasing $\widetilde{\sigma}$ and for $a \geq 1.2$, the quantity $\alpha(\widetilde{\sigma})$ decreases. This result is worth to be emphasized. In reference [21] the B contribution term to equation (8) has been interpreted as the turbulent part leading to anomalous bunch lengthening and energy spread, while in references [13,23], to explain the experimental results, it was assumed that the turbulent part was decreased by the FEL interaction, as confirmed by the present investigation.

The equilibrium output power can be evaluated as before with the only difference that the stationary intracavity dimensionless power is provided by

$$R(x)\left[1 + 1.7\mu_\varepsilon^2(0)\Sigma(X)^2\right] = \frac{1}{r}\,. \tag{14}$$

The corresponding efficiency function is given in Figure 8, and in this case too larger values correspond to an operation affected by the corrections of equations (9).

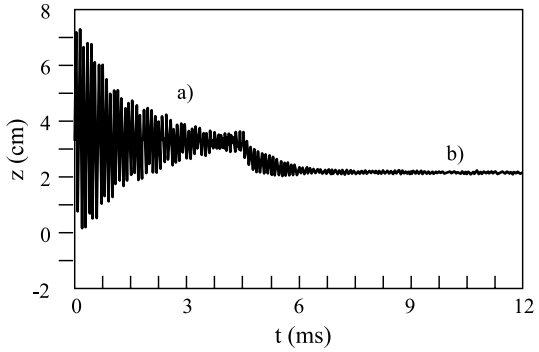

Fig. 10. Position of the longitudinal bunch centroid *vs.* time. a) Evolution dominated by Microwave Instability only. b) FEL interaction switched on at 4.5 ms. The FEL power corresponds to the threshold value sufficient to suppress the instability, without inducing additional energy spread growth.

4 Concluding remarks

We consider important, for a more complete understanding of the FEL-Microwave instability interplay, to point out that the mechanism leading to the anomalous bunch lengthening are not different from those underlying the FEL dynamics itself. When the peak current exceeds a certain limit the instability may grow but it in turn determines an increase of the energy spread and bunch length, when the peak current is reduced the instability does not grow any more and the anomalous part of the energy spread is reduced by radiation damping effects. When the original peak current values are restored the mechanism may start again. It is evident that any effect providing further energy spread may act as a feedback element for the microwave instability.

This statement is further supported by Figure 9, where we have reported induced energy spread *vs.* $\widetilde{\sigma}$ for the cases with and without anomalous bunch lengthening effects. It is evident that when $\widetilde{\sigma}$ increases, there are not appreciable differences between the two cases. This result is particularly interesting also because reproduces an analogous calculation of reference [13] where the effects of the instability

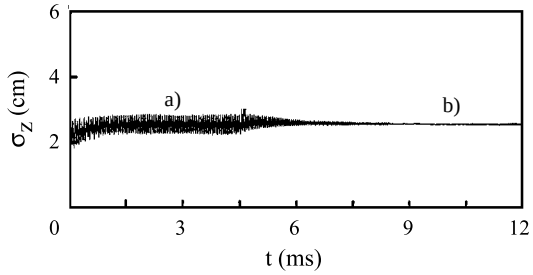

Fig. 11. Same as Figure 10 for the r.m.s. bunch length.

have been modeled using a totally numerical procedure, based on a ray-tracing analysis of the longitudinal phase space evolution.

A more transparent insight is provided by Figure 7 which allows the conclusion that the anomalous part of the bunch lengthening vanishes with increasing intracavity power and thus with increasing induced energy spread.

The results of this paper confirm in a more quantitative way the suggestion put forward in previous investigations, according to which the onset of the FEL allows the conditions to switch off the instability. The induced energy spread causes, indeed, a bunch lengthening, which in turn reduces the peak current and thus the coupling with the SR environment, which eventually determines a reduction of the loss power efficiency. Within the present context, the above-described phenomenology, can be traced back to the basic assumption of the model according to which the anomalous part of the energy spread is depending on the wake-field intensity, which in turn is linked to the total bunch length. An increase of the bunch length leads to a reduction of the wake field emission efficiency.

The agreement between the present results and those of reference [13] is important because it confirms the possibility of describing, by employing a toy model and a fairly modest computational effort, a feedback mechanism which may have an important impact in the development of SR-FEL sources and also for the design of SR with high brightness and low intrinsic noise. An example is provided by Figures 10, 11 where we have reported the evolution calculated with a numerical code of the electron e-bunch center of mass and r.m.s. length, under the influence of microwave instability and FEL interaction. The particularly noisy behaviour is counteracted by the onset of a low-intensity FEL which significantly reduces the noise, without providing additional effects.

Appendix

In the previous Sections we have used dimensionless variables, which will be specified in this appendix for completeness.

The Haissinski equation, in the propert units and under appropriate conditions reads

$$\sigma_z^3 - \sigma_{z,0}^2\sigma_z - \lambda I_0 \frac{z_i}{n} = 0\,, \tag{A.1}$$

where

$$\lambda = \frac{\alpha_c c^2 L_c}{(2\pi)^{3/2}\omega_s^2\left(\dfrac{E_0}{e}\right)}\,, \tag{A.2}$$

with I_0 being the bunch average current, z_i/n the normalized impedance, α_c the momentum compaction, ω_s the synchrotron frequency, L_c the machine length and E_0 the nominal machine energy. By using typical values we obtain

$$\lambda \sim 7.3\cdot 10^{-4}[\mathrm{m^3 eV^{-1}}]\,. \tag{A.3}$$

By assuming furthermore z_i/n of the order of few Ω, I_0 of few tens of mA and $\sigma_{z,0}$ of the order of centimeters, we find that $\bar{A} = \frac{\lambda I_0 z_i/n}{\sigma_{z,0}^3}$ is of the order of unity. This justifies the values we have used in the numerical examples.

The equations valid in the microwave instability regime should read as

$$\begin{aligned}
&\sigma_z^3 - \sigma_{z,0}^2\sigma_z\left[1+\ell_1 I_0^2 k_e^2(\sigma_{z,0})\left(\frac{\sigma_{z,0}}{\sigma_z}\right)^{2a}\right] - \lambda I_0\frac{z_i}{n} = 0,\\
&\sigma_\varepsilon^2 - \sigma_{\varepsilon,0}^2\left[1+\ell_1 I_0^2 k_e^2(\sigma_{z,0})\left(\frac{\sigma_{z,0}}{\sigma_z}\right)^{2a}\right] = 0\,,
\end{aligned} \tag{A.4}$$

where

$$\ell_1 = \frac{144\varepsilon_0 L_c^2\rho^2}{55\sqrt{3}\hbar c^3\gamma^7}\,, \tag{A.5}$$

$k_e(\sigma_{z,0})$ is the loss factor and ρ the bending radius, the use of typical reference numbers provides for values ranging between 10^0 and 10^2.

References

1. A. Renieri, Nuovo Cimento B **53**, 160 (1979).
2. N.A. Vinokurov, A.N. Skrinsky, preprint 77-67 of the institute of Nuclear Physics, Novosibirsk (1977).
3. G. Dattoli, A. Renieri, Nuovo Cimento B **59**, 1 (1980).
4. M. Billardon *et al.*, Phys. Rev. Lett. **51**, 1652 (1983).
5. J.B. Drobyazko *et al.*, Nucl. Instrum. Methods A **282**, 424 (1989).
6. V. Litvinenko, Nucl. Instrum. Methods A **407**, 8 (1988).
7. P. Elleaume, IEEE J. Quantum Electron. **21**, 1012 (1985).
8. G. Dattoli, A. Renieri, A. Torre, J.C. Gallardo, Phys. Rev. A **35** 4175 (1987); G. Dattoli, T. Hermsen, A. Renieri, A. Torre, J.C. Gallardo, Phys. Rev. A **37**, 4326 (1988); G. Dattoli, T. Hermsen, L. Mezi, A. Renieri, A. Torre, Phys. Rev. A **37**, 4134 (1988).
9. M.E. Couprie, Nucl. Instrum. Methods A **393**, 13 (1997).
10. M.E. Couprie *et al.*, *Proceedings of the Third PAC Conference, Berlin 1992*, edited by H. Henke, H. Homeyer, Ch. Petit-Jean-Genaz (Edition Frontières, Berlin, 1992) p. 623.
11. A.M. Sessler, Lawrence Berkeley Report No. 28, 1973 (unpublished).
12. A. Chao, *Physics of Collective Beam Instabilities in High Energy Accelerators* (J. Wiley and Sons, New York, 1993).

13. G. Dattoli, A. Renieri, G.K. Voykov, Phys. Rev. E **55**, 2056 (1997).
14. G. Dattoli *et al.*, Phys. Rev. E **58**, 6570 (1998).
15. G. Dattoli, L. Mezi, P.L. Ottaviani, A. Renieri, M. Vaccari, Phys. Rev. E **57**, 7161 (1998).
16. P. Elleaume, J. Phys. (Paris) **45**, 997 (1984).
17. G. Dattoli, L. Giannessi, P.L. Ottaviani, A. Renieri, Nucl. Instrum. Methods A **365**, 559 (1995).
18. M. Sands, Stanford Linear accelerator - Report Nbo. SLAC-121, 1970 (unpublished).
19. J. Haissinski, Nuovo Cimento B **18**, 72 (1973); A. Hofmann, J. Maidment, CERN-LEP/TH-88-51, 1988.
20. A. Renieri, Laboratori Nazionali di Frascati, Report LNF/101(R) 1975 (unpublished).
21. K. Wille, Nucl. Instrum. Methods A **393**, 18 (1997).
22. J. Gao, *Bunch-lengthening and energy spread increasing in Electron Storage Rings, Particle Accelerator Conference* (APS, 1997).
23. G. Dattoli, L. Mezi, A. Renieri, G.K. Voykov, Nucl. Instrum. Methods A **393**, 70 (1997).